THE ROYAL SOCIETY

Uniformity, specificity and variability of corticocortical connectivity

Claus-C. Hilgetag[1*] **and Simon Grant**[2]

[1]*Neural Systems Group, Departmen of Psychology, University of Newcastle upon Tyne, Ridley Building, Newcastle upon Tyne NE1 7RU, UK*

[2]*Department of Sensorimotor Systems, Division of Neuroscience, Imperial College School of Medicine, Charing Cross Campus, Fulham Palace Road, London W6 8RF, UK*

In many studies of the mammalian brain, subjective assessments of connectivity patterns and connection strengths have been used to subdivide the cortex into separate but linked areas and to make deductions about the flow of information through the cortical network. Here we describe the results of applying statistical analyses to quantitative corticocortical connection data, and the conclusions that can be drawn from such quantitative approaches.

Injections of the tracer WGA-HRP were made into different visual areas either side of the middle suprasylvian sulcus (MSS) in 11 adult cats. Retrogradely labelled cells produced by these injections were counted in selected coronal sections taken at regularly spaced intervals (1 mm) through the entire visual cortex, and their cumulative sums and relative proportions in each of 16 recognized visual cortical areas were computed. The surface dimensions of these areas were measured in each cat, from contour lines made on enlarged drawings of the same sections. A total of 116 149 labelled neurons were assigned to all visual cortical areas in the 11 cats, with 5212 others excluded because of their uncertain location. The distribution of relative connection strengths, that is, the percentage of labelled cells per cortical area, was evaluated using non-parametric cluster analyses and Monte Carlo simulation, and relationships between connection strength and area size were examined by linear regression.

The absolute size of each visual cortical area was uniform across individual cats, whereas the strengths of connections between the same area pairs were extremely variable for injections in different animals. The overall distribution of labelling strengths for corticocortical connections was continuous and monotonic, rather than inherently clustered, with the highest frequencies presented by the absent (zero density) and the very-low-density connections. These two categories could not, on analytical grounds, be separated from each other. Thus it seems that any subjective description of corticocortical connectivity strengths by ordinal classes (such as 'absent', 'weak', 'moderate' or 'strong') imposes a categorization on the data, rather than recognizes a structure inherent in the data themselves.

Despite the great variability of connections, similarities in the distribution profiles for the relative strengths of labelled cells in all areas could be used to identify clusters of different injection sites in the MSS. This supported the conclusion that there are four connectionally distinct subdivisions of this cortex, corresponding to areas 21a, PMLS and AMLS (in the medial bank) and to area PLLS (in the lateral bank). Even for tracer deposits in the same cortical subdivision, however, the strength of connections projecting to the site from other cortical areas varied greatly across injection in different individual animals. We further demonstrated that, on average, the strength of connections originating from any given cortical area was positively and linearly correlated with the size of its surface dimensions. When analysed by specific injection site location, however, this relationship was shown to hold for the individual connections to the medial bank MSS areas, but not for connections leading to the lateral bank area. The data suggest that connectivity of the cat's visual cortex possesses a number of uniform global features, which are locally organized in such a way as to give each cortical area unique characteristics.

Keywords: cats; visual cortex; lateral suprasylvian; connection strengths; Monte Carlo simulation; non-parametric clustering

1. INTRODUCTION

Many models of information processing in the mammalian cortex are based on selected organizational features of long-range corticocortical connectivity, as revealed by neuroanatomical pathway tracing techniques (e.g. Zeki & Shipp 1988; Van Essen *et al*. 1992; Young 1992; Scannell *et al*. 1995). Fundamental to these models, regardless of whether they emphasize the parallel, hierarchical or network characteristics of the underlying connectivity, is the belief that the cortex consists of specialized, separate areas, which can also be identified on the basis of their

*Author and address for correspondence: Boston University School of Medicine, Department of Anatomy and Neurobiology, 700 Albany Street W746, Boston, MA 02118, USA (claush@bu.edu).

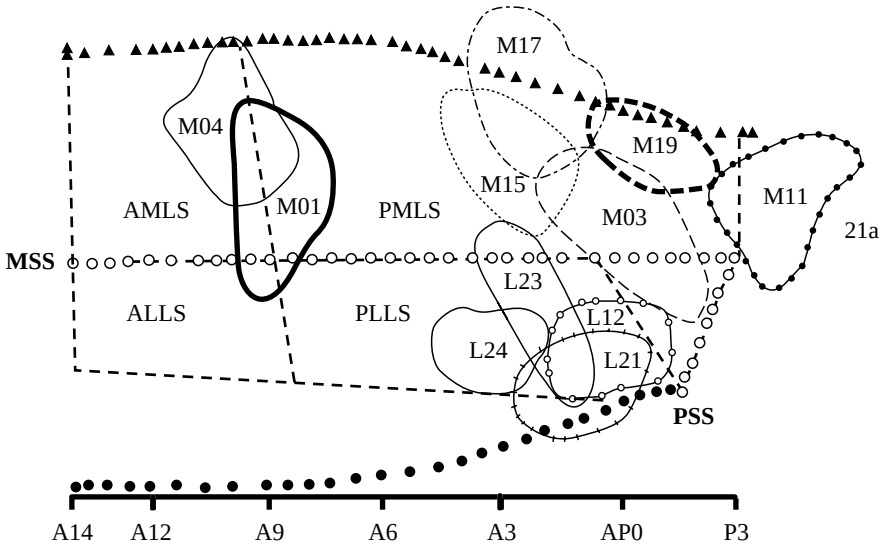

Figure 1. Distribution and extent of tracer injection sites. The diagram schematically shows the 11 injection sites and the assumed boundaries of areas 21a, MLS, AMLS, PMLS and ALLS on a flattened surface map of the cortex, in relation to the middle suprasylvian sulcus (MSS) and the posterior suprasylvian cortex (PSS). The left-to-right orientation of the map corresponds to an anterior-to-posterior order of the evaluated sections.

unique complement of cortical connections. Major significance is usually attributed to distinctions in the strength of connections between each cortical area and other specialized cortical regions (e.g. Lennie 1998). Unfortunately, very few attempts have been made to study the anatomy of corticocortical connections in a quantitative manner (but see Sherk 1986; Musil & Olson 1991; Barone *et al*. 1995; Lomber *et al*. 1995; MacNeil *et al*. 1997). The rarity of such approaches is, however, understandable, given the enormous number of connections that can be labelled by modern anatomical tracing methods and the lack of automated techniques for their subsequent evaluation. Nonetheless, an urgent need for greater quantification of cortical connectivity exists, so that the cornerstones underlying current models of information processing can be exposed to more critical appraisal.

This requirement is typified by previous studies of the cortical areas surrounding the middle suprasylvian sulcus (MSS) of cat extrastriate cortex. This sulcus contains a complex of areas dedicated to different aspects of visual motion analysis, perhaps analogous to the superior temporal sulcus in Old World monkeys (Shipp & Grant 1991; Payne 1993), but their number, boundaries and relationships to each other remain matters of dispute. Based on physiological visual field mapping, Palmer *et al*. (1978) suggested that the MSS possesses four major subdivisions: a large posterior and smaller anterior area in its medial bank (areas PMLS and AMLS, respectively) and two similarly situated areas in the lateral bank (PLLS and ALLS; see § 2 for abbreviations of area names). These suggestions gained subsequent support from a comprehensive connectional mapping study, indicating that the strength of connectivity between these areas and other areas of the visual cortex differed sufficiently for each subdivision to be considered unique (Symonds & Rosenquist 1984*a*). Others, however, have argued on the basis of an almost identical experimental approach that AMLS, PMLS and area 21a (immediately caudal to PMLS) share common corticocortical connectivity strengths, and so should be considered parts of a single subdivision of the lateral suprasylvian (LS) visual cortex (Sherk 1986; Grant & Shipp 1991). These studies relied mainly on subjective assessments of connectional data, and also on the assumption that constancy of connection strength allows a reliable identification of areas. These conclusions as well as the underlying assumptions, however, are called into question by recent quantitative analyses of connectivity associated with just a small subregion of area PMLS, which demonstrated that the strength of this region's cortical connections can vary markedly between individual animals (MacNeil *et al*. 1997). Here we re-evaluate the organization of the MSS region and its connectivity using systematic statistical analyses of quantitative neuroanatomical data.

2. METHODS

This paper analyses the labelling of cortical neurons resulting from injections of the dye WGA-HRP into the lateral suprasylvian region of the cat visual cortex. Data from injections in 11 cats entered the analyses. The distribution and extent of the injection sites are shown in figure 1. A detailed description of the procedures for injecting the dyes and preparing the tissue is given elsewhere (Grant & Shipp 1991). The injected brains were serially sectioned at 60 µm thickness in the coronal plane, from the occipital pole to the anterior commissure. The sections were divided into four series, at least two of which were processed to reveal the labelling by WGA-HRP histochemistry (Grant & Shipp 1991). Other sections were stained for Nissl cell bodies or acetylcholinesterase (Graybiel & Berson 1980) to show the laminar and cellular morphology. The WGA-HRP-labelled sections were examined under both bright- and darkfield microscopy, and large-scale camera-lucida drawings were produced, plotting the location of labelled cells and terminals.

Based on anatomical landmarks (the position relative to sulci and gyri), previously described cortical areas were identified in the sections and marked on the section drawings. Most of the WGA-HRP labelling found in the sections could be assigned to one of the following 16 areas: 17, 18, 19, 20a, 20b, PS (posterior suprasylvian), 21a, 21b/VLS (ventrolateral suprasylvian), DLS/Peg (dorsolateral suprasylvian/posterior ectosylvian gyrus), PMLS (posteromedial lateral suprasylvian), PLLS (posterolateral

lateral suprasylvian), AMLS (anteromedial lateral suprasylvian), ALLS (anterolateral lateral suprasylvian), 7p, SVA (splenial visual area) or AEV (anterior ectosylvian visual area). A good introductory survey of these and other cat cortical areas can be found in Scannell *et al*. (1995).

To determine the absolute and relative sizes of the identified areas, a line running through the middle of the grey matter (approximating layer 4) and following the contours of all gyri and sulci was added to every section drawing. The length of the contour line was measured in each of the cortical areas present in the sections. Given a standard interval of 1 mm between the sections, we assumed each section to represent the average of the whole region 0.5 mm anterior and 0.5 mm posterior to it. The total surface dimensions of each cortical area were, therefore, estimated by adding the lengths of every contour line drawn through the given region and multiplying this value by the 1 mm of averaged thickness. To measure the lengths, the contour lines were traced on a digitizing tablet linked to a PC, using the Sigma-Scan software (Jandel Scientific).

Labelled cells were counted under a light microscope (×40/ ×100 total magnification) in the same sections as represented in the diagrams, that is, at 1 mm intervals. Large numbers of cells in the sections, and any conspicuous constellations, were recounted until a within- or between-observer accuracy of ±5% had been reached (for two observers). Additionally, the distribution of labelled terminals in the processed sections was estimated. The following analyses will, however, focus on the distribution of retrograde label, as the latter could be more easily and accurately determined. Between 25 800 (for case M11) and 4724 (for case L24) labelled cells were counted for the 11 individual injections, of which between 1.32% (M15) and 8.75% (M04) could not be reliably assigned to particular visual cortical areas.

In line with the terminology used by Scannell *et al*. (this issue), we refer to connections unravelled by tracer injections in the same individual animal as 'intra-animal' connections, whereas connections uncovered by injections in different animals are referred to as 'inter-animal'. Consequently, the present analyses derive conclusions about the features of inter-animal connections, as the data are based on one injection per animal, and these connectional features may be influenced by a range of factors within the individual animal as well as within the whole population. We describe the statistical methods used for analysing the data and the results obtained in the relevant sections of this paper.

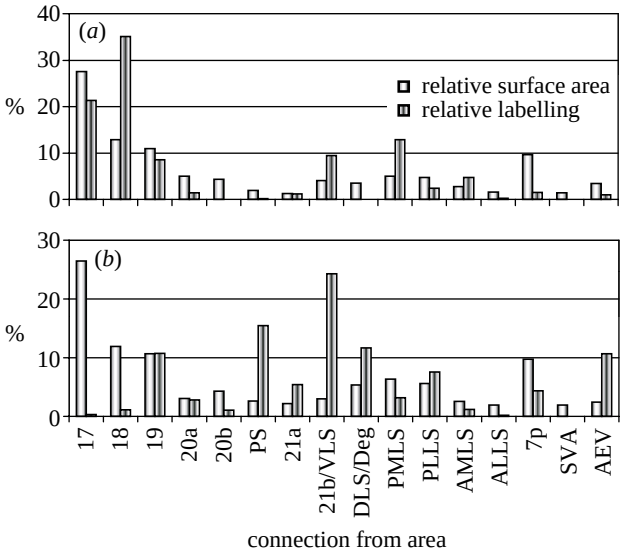

Figure 2. Profiles for the distribution of retrograde label following two different injections in cat LS cortex. Shown are injection cases (*a*) 'M15' and (*b*) 'L21'. The diagram gives the relative distribution of label (connection density) and the relative size of the area from which the connection originated. While the relative area sizes are very similar in the two cases, the connection densities differed greatly.

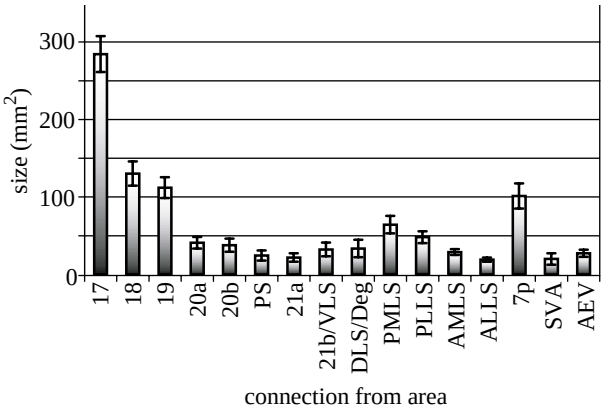

Figure 3. Absolute sizes of 16 cat cortical areas (in mm^2) averaged across 11 individual cases. The error bars represent ±1 s.d.

3. RESULTS

(a) *Constancy of area sizes and variability of connection densities*

The assignment of retrogradely labelled cells to different areas allowed the creation of label distribution profiles for each of the 11 injections. Two such profiles are shown in figure 2, in which the relative surface dimensions of areas and the respective proportions of the total cell labelling (which we refer to as relative densities) are given for a medial and a lateral bank injection.

Figure 2 shows that the relative area sizes were constant in those two cases. Figure 3, giving the absolute sizes of each individual area for all 11 animals, demonstrates that this was a consistent feature across individuals. The average surface area sum of all 16 areas was 1027 mm^2 (with a standard deviation of 100 mm^2, or a standard error of 30 mm^2), of which the largest (area 17) consistently accounted for 26–30%, whereas smaller areas such as SVA, ALLS or 21a contributed only some 1–3%. The surface dimensions obtained for area 17 (mean 284 mm^2, standard error 7 mm^2) were significantly smaller than the value of 380 mm^2 previously reported by Tusa *et al*. (1978) from *in vivo* measurements in adult cats. This discrepancy could be explained by a 10–15% shrinkage of our fixed and histochemically processed material. The consistency of area sizes emerged even though the area boundaries were specified only with respect to gross anatomical landmarks. This finding may also indicate a more general invariance of cortical dimensions and of the arrangement of main cortical landmarks in the cat.

All subsequent analyses focused on the relative, rather than absolute, connection densities, as the latter are strongly influenced by several experimental factors, such as the volume of tracer injected and the efficiency of its uptake, as well as the particulars of the tissue processing and the counting process (Coggeshall & Lekan 1996).

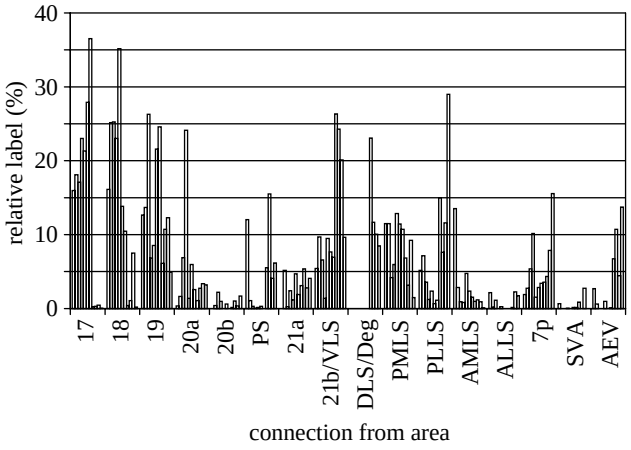

Figure 4. Variation of relative anatomical connections strengths for injections of retrograde tracer into the medial and lateral bank of the LS cortex in 11 individual cats. The bars represent the relative amount of labelling, as described in the text. The different injection cases are plotted in the order: M01, M03, M04, M11, M15, M17, M19, L12, L21, L23, L24.

The relative number of labelled cells, on the other hand, should be much less affected by these factors and so provide more consistent information on connection strengths. As shown in figure 4, however, the relative densities of connections between other visual cortical areas and the LS region varied dramatically across the individual cases. In the next sections, we analyse factors related to this surprising connectional variability.

(b) *Regional parcellation based on connectivity profiles*

Within the scope of our study, which draws on a distribution of inter-animal connections, the observed variability of densities can be due both to factors contributing to the variation of densities within an individual animal and to additional differences between individuals in the population. We first investigated the possibility that some part of the inter-animal connectional variability might be attributable to the placement of tracer into different areas of the LS complex. In that case, what appears to be variability, may arise only from pooling together injections that were made into disparate cortical subdivisions with different connectivity profiles. This source of variation can be reduced by grouping the different injection cases on the basis of similarities in their labelling profiles. The resulting grouping of cases can, moreover, be used to conclude that the respective injections were made in the same cortical subdivisions. Such a criterion of differential connectivity has been used frequently to distinguish between neighbouring cortical regions (Van Essen 1985; Sherk 1986).

It is apparent from figure 4 that, although the distribution of relative connection densities covers a wide range, the majority of densities are low (between 0% and 5%), so that their distribution is strongly skewed. To spread the data more equally across a metric scale and to avoid misinterpretations of the density distribution, the relative densities, x, were converted by a logarithmic transform $\ln(x + 1)$.

To look for similar profiles in the transformed data, we performed a non-parametric cluster analysis (NPCA) of the transformed values, using the MODECLUS procedure of the SAS statistical software (SAS Institute, Inc.). Briefly, NPCA seeks to identify the proximity and grouping of data points in an n-dimensional metric coordinate space by estimating the density distribution of the data points throughout the space. The estimate is based on either a specified number of data points or a given radius within which data points might be found. For the present case, the problem was to find the proximities of the 11 different injection cases, based on their profiles of label distribution in 16 areas. These profiles could thus be considered as coordinates in a 16-dimensional coordinate space. Since it is impossible to visually display the clustering of points in the 16-dimensional space, the cluster results are given in series of tables outlining the number and composition of clusters resulting from different MODECLUS parameter settings (table 1).

We used three different methods, provided by the SAS software, of estimating the density distribution of the coordinate points. The first method based the estimate on the given number of nearest neighbours, K, for any data point. The latter two methods used set radii, R, for the cluster-density estimation. Whereas the second method allowed clusters consisting of just one injection case, the third method required that at least two injections be found in any cluster. For both these methods, kernel radii were varied by increments of 0.25. The results of the different computations are presented in table 1*a–c*.

The results of all three computational approaches consistently demonstrated that the injections could be grouped into two principal clusters, corresponding to injections into the medial, 'M', and into the lateral bank, 'L', of the MSS cortex. One could, therefore, distinguish two general categories of injections, or assign the injections to two broad regional subdivisions.

The results from the second clustering approach, shown in table 1*b*, suggest further differentiation of these regions. Reducing the clustering radius to exclude the most dissimilar cases led to the separation of the injections M01, M04, M11 from the general division of 'M' and 'L' cases, at a radius $R = 4$. Inspecting the distribution of injection sites (figure 1), it is notable that the injections making up the most stable 'M' cluster (consisting of M03, M15, M17 and M19) were adjacent and overlapping, in the caudal medial bank of the MSS. Similarly, the four stable 'L' cases (L12, L21, L23 and L24) were also in close spatial proximity in the lateral bank of the MSS. The remaining three injections that form individual clusters were M11, situated caudally and non-overlapping with the other medial bank injections, and partly overlapping injections M01 and M04, situated far rostrally in the medial bank (figure 1).

Reducing the radius further (at R between 2.75 and 3) separated the 'L' cases, which signals that the injection cases that make up the 'L' cluster are more dissimilar among each other than the four cases that form the stable 'M' cluster. Moreover, it can be seen that the four injection cases M03, M15, M17 and M19 are more similar to each other than the remaining injections, which separate into individual clusters. This indicates that spatial proximity and overlap of the injections did not necessarily lead to similar labelling profiles. While table 1*c* also supported the clear distinction between medial and

Table 1. *Cluster structure of injection cases by connection density profiles*

(The independent parameter is given in the first column, the resulting cluster number and structure in the second and third column, respectively.)

(*a*) *Clustering injection profiles with K-nearest-neighbour density estimates*

number of nearest neighbours (K)	number of clusters	cluster structure
<5	2	{M01, M03, M04, M11, M15, M17, M19}, {L12, L21, L23, L24}
$\geqslant 5$	1	{M01, M03, M04, M11, M15, M17, M19, L12, L21, L23, L24}

(*b*) *Clustering injection profiles using uniform kernel density estimates (with kernel radius R ranging between the values given in the first column)*

radius (R)	number of clusters	cluster structure
<2	11	{M01}, {M03}, {M15}, {M04}, {M11}, {M17}, {M19}, {L12}, {L21}, {L23}, {L24}
2–2.5	10	{M17, M19}, {M01} , {M03}, {M04}, {M11}, {M15}, {L12}, {L21}, {L23}, {L24}
2.75–3	8	{M03, M15, M17, M19}, {M01} , {M04}, {M11}, {L12}, {L21}, {L23}, {L24}
3.25–3.75	7	{M03, M15, M17, M19}, {L12, L21}, {M01} , {M04}, {M11}, {L23}, {L24}
4	5	{M03, M15, M17, M19}, {L12, L21, L23, L24}, {M01} , {M04}, {M11}
4–5	2	{M01, M03, M04, M11, M15, M17, M19}, {L12, L21, L23, L24}
$\geqslant 5$	1	{M01, M03, M04, M11, M15, M17, M19, L12, L21, L23, L24}

(*c*) *Clustering using uniform kernel density estimates (with kernel radius R)*

(This approach is very similar to the one that produced the results shown in table 1*b*. Here, however, the clustering neighbourhoods extended to the second nearest neighbour (MODECLUS parameter $CK=2$). This means that any cluster had to contain at least two elements.)

radius (R)	number of clusters	cluster structure
1.5–2.5	3	{M01, M03, M15}, {M04, M11, M17, M19}, {L12, L21, L23, L24}
2.75–5	2	{M01, M03, M04, M11, M15, M17, M19}, {L12, L21, L23, L24}
>5	1	{M01, M03, M04, M11, M15, M17, M19, L12, L21, L23, L24}

Table 2. *Assignment of injection cases to cortical areas based on profiles of label distribution*

injections	assigned to area
M11	21
M04	AMLS
M01, M03, M15, M17, M19	PMLS
L12, L21, L23, L24	PLLS

lateral bank cases, it suggested a different grouping of some 'M' cases for low clustering radii. Interestingly, the grouping of these injection sites appears to be based on their depth in the MSS with M01, M03 and M15 close to the fundus of the sulcus, and M04, M11, M17 and M19 further up. However, this particular clustering approach might suffer from the additional constraint that any cluster had to be made up from at least two individual cases.

Based on their close relative similarity, we assigned the caudal medial injections M03, M15, M17 and M19 to area PMLS and the caudal lateral injections L12, L21, L23 and L24 to area PLLS. Medial case M01, which spatially overlapped with the injection M04 (figure 1), was nevertheless dissimilar to it in all reduced-radii clustering configurations, indicating that the placement of tracer was made into a different cortical area. The only likely possibility was that M01 belonged to area PMLS, even though it separated from the other PMLS cases for most of the reduced-radii clusters. Palmer *et al*. (1978) have suggested on the basis of visual field mapping that PLMS may consist of rostral and caudal subdivisions with differential visuotopic organization, which could explain this discrepancy (also see § 4). Similarly, case M04 most likely involved area AMLS, and the very caudal injection (case M11), which also was dissimilar from the main PMLS cases, was assumed to be located in another distinct cortical region, corresponding to area 21a. Table 2 summarizes the assignment of the 11 injection cases to four different cortical areas.

The variability of the relative densities was reduced by grouping them according to the injected area. The standard deviation of densities within the cases assigned to area PMLS was, on average, reduced by 43%, and within the PLLS cases by 23%, compared to the standard deviation of the same connections across all injections. The difference between the two groups again indicated the larger dissimilarity of the lateral bank cases. However, there remained considerable variability even within the cases that had been brought together by the similarity of their connection density profiles. Figures 5 and 6 show this intra-group variation for the compiled injection cases PMLS and PLLS, respectively, and demonstrate that the standard deviation of the connection densities for many areas remained equal to or greater than their means. Thus, the great variability of inter-animal connections may not be fully explained by injection site location. We consider alternative explanations in § 4.

(c) *Density of corticocortical connections*

As individual corticocortical connections possess considerable variability and are difficult to characterize

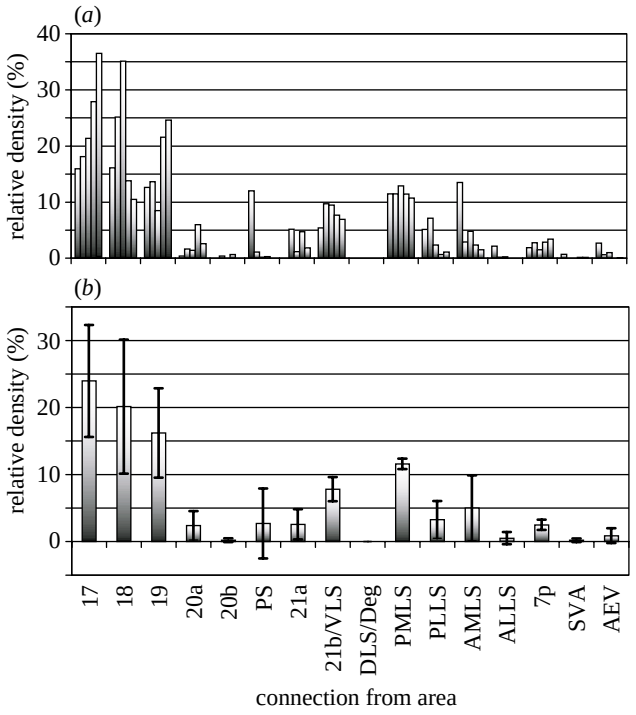

Figure 5. Variation of density in the connections terminating in cortical area PMLS, identified by five different inter-animal injections. (*a*) The injections are displayed in the order M01, M03, M15, M17 and M19. (*b*) Average connection density values for the five connections. The error bars represent ± 1 s.d.

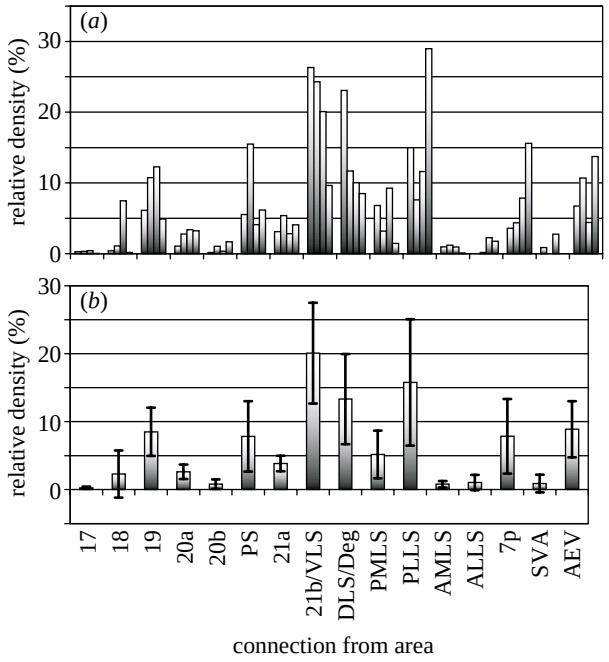

Figure 6. Variation of density in the connections terminating in cortical area PLLS, identified by four different inter-animal injections. (*a*) The injections are displayed in the order L12, L21, L23, L24. (*b*) Average connection density values for the connections. The error bars represent ± 1 s.d. It is noteworthy that the intrinsic connectivity, which is marked by label uptake outside the injection side, but within the injected cortical area, appears to be much more variable within area PLLS than within PMLS.

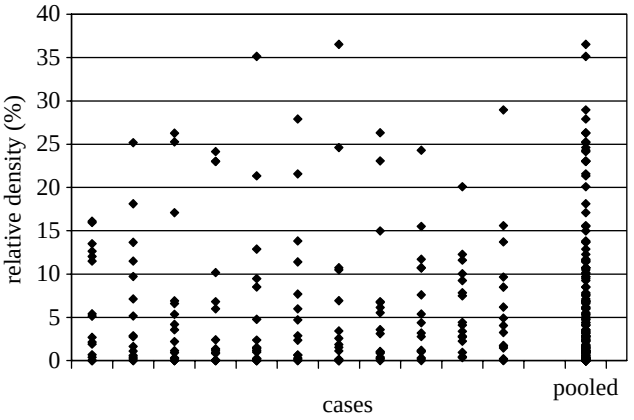

Figure 7. Scatter plot of relative label distributions for all injection cases. From left to right, the cases are M01, M03, M04, M11, M15, M17, M19, L12, L21, L23, L24, as well as the pooled data from all of the single cases.

by a unique value, we wondered whether they could be fitted into broad descriptive categories of connection strength. Categories such as 'weak', 'intermediate' or 'strong' have been used frequently in the anatomical literature (e.g. Symonds & Rosenquist 1984*a*; Grant & Shipp 1991; Scannell *et al.* 1995) and in modelling studies (e.g. Hilgetag *et al.* 1999) to characterize the magnitude of connections. The data presented in figures 5 and 6 appear to suggest that some individual connections cannot even be confined to such wide ordinal classes. Consider, for example, the connection originating in area 19 and terminating in area PMLS (figure 5), which in one instance has a relative density of well below 10% ('weak' to 'intermediate'?), but in another case of 25% ('strong'?). Similarly, the connection from area PS to PMLS is all but absent in most cases, although it rises to about 12% ('intermediate'?) in one instance.

How can the strength of a particular corticocortical connection (that is, between the same pair of cortical areas in different animals) be defined reliably? How many descriptive classes would be needed, and how should they be defined? To approach this problem, we first looked for inherent classes or clusters in the distribution of all connection densities. In the absence of such clusters, one would have to conclude that the distribution of densities is continuous and hence non-categorical. Figure 7 gives a scatter plot for the relative connection densities in all individual, and in the pooled, injection cases. It is clear that the majority of densities was small (less than 5%) or non-existent and that some of the distributions for single projections appeared to be grouped in a small number of clusters. For example, in most cases, the majority of connections formed a relatively compact group, whose members possessed less than 15% of the relative label, while only a few singular connections were stronger than this.

The pooled distribution of all cases, however, appears more continuous, and it is not obvious how general density classes could be defined from these data. As before, we transformed the pooled connection densities logarithmically to account for the skewed and wide-ranging distribution of data points, using a transform $y_i = \ln(x_i + 1)$, where x_i is the original and y_i the

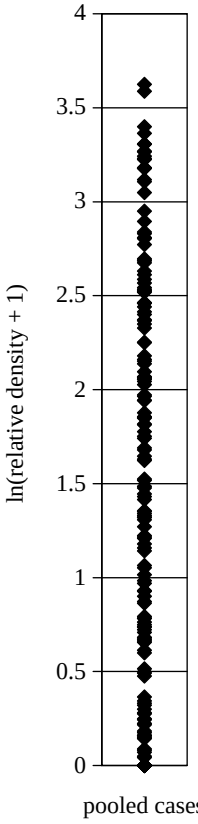

Figure 8. Scatter plot of the logarithmically transformed pooled connection densities from figure 7.

transformed ith connection strength. (A simple $\ln(x_i)$ transform would have yielded difficulties in the cases where $x_i = 0$.) The result of the transform is displayed in figure 8, which demonstrates that the distribution of connection densities is more homogeneous than first assumed. All following analyses are based on the transformed distribution.

We next plotted the distribution of connection densities in frequency histograms with various bin widths. Figure 9 shows a frequency histogram with bin width 0.1. This bin setting provided a good compromise between showing the distribution in sufficient detail and leaving most of the bins filled. If distinct classes of densities existed in this distribution, these classes should be separated significantly by empty bins or bins with only very few members. Even if such classes were found in the data, it also had to be established whether a similar arrangement could have arisen by chance, simply by random sampling from a smooth monotonic or unimodal gradient of densities. We tested the latter possibility by pursuing a systematic simulation approach (that is, a Monte Carlo simulation). The approach proceeded by fitting a simple theoretical distribution to the experimental distribution. Different random samples were then drawn from the theoretical distribution and were compared with results from the actual data.

We used the freeware program PeakFitter (v. 1.1) to approximate the distribution of experimental data with a continuous and monotonic function. To account for both the high peak at zero and the remainder of the distribution in a simple way, we used a combination of a hyperbolic function and a constant, $f(x) = c_1/x + c_2$ (where c_1 and

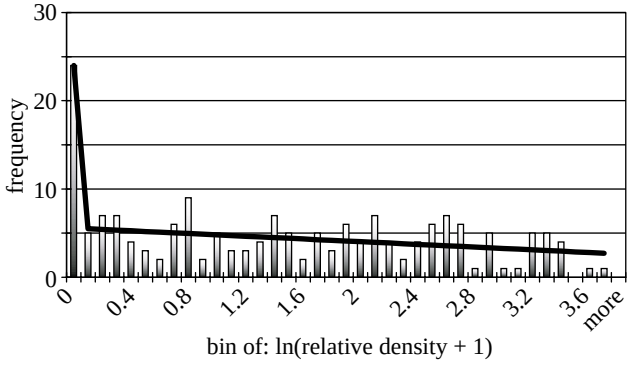

Figure 9. Frequency histogram of the distribution of densities shown in figure 8. Bin width = 0.1. The superimposed curve derives from fitting the histogram values x with a monotonic gradient, which has the function $c_1/x + c_2x + c_3$. The constants are those whose settings are given in the main text.

c_2 are constants). To account also for the decrease of frequency with increasing x, we added a further linear component. The resulting fitting function $f(x)$ was

$$f(x) = c_1/x + c_2x + c_3. \quad (1)$$

The values of the constants were determined by PeakFitter as $c_1 = 1.843 \times 10^{-5}$, $c_2 = -0.7705$ and $c_3 = 5.572$. This curve fit, which is superimposed on the histogram in figure 9, produced a standard error of 1.977 measured against the binned frequencies of the density distribution. In ten different trials, we sampled 176 random data points from this distribution (that is, the same number as there were actual values), accounting for the standard error of the curve fit by probabilistic sampling according to a normal distribution around the curve. The method of sampling made sure that the average distribution of the simulated connection densities was identical to that of the real data.

We analysed both the experimental and the simulated distributions with non-parametric cluster analysis. The data, in this case, were considered as coordinate points along a one-dimensional axis, and the clustering technique evaluated their distribution in metric space on the basis of different given parameters, as outlined briefly in § 3(b). We again used the three clustering approaches provided by the SAS MODECLUS routine as well as a wide range of parameters for the cluster-density estimation. The parameters ranged from $K = 20$ to $K = 60$ (at increments of 2) for the Kth nearest-neighbour clustering and from $R = 0.1$ to $R = 7.5$ (at increments of 0.05) for the fixed kernel clustering approaches. Inspection of the clusters obtained for experimental and simulated data made it clear that the two sets were indistinguishable in most respects, as exemplified by figure 10, which presents cluster configurations proposed for (*a*) the experimental and (*b*) simulated data. We statistically compared the number of clusters obtained by the clustering procedures for real and simulated data. For 41 out of the 49 different MODECLUS parameter settings, the number of clusters for the experimental data was contained in the normal distribution defined by the number of clusters for the ten simulated data sets, and for the remaining eight settings no consistent trends were evident. Therefore, the experimental data were no more clustered than would be

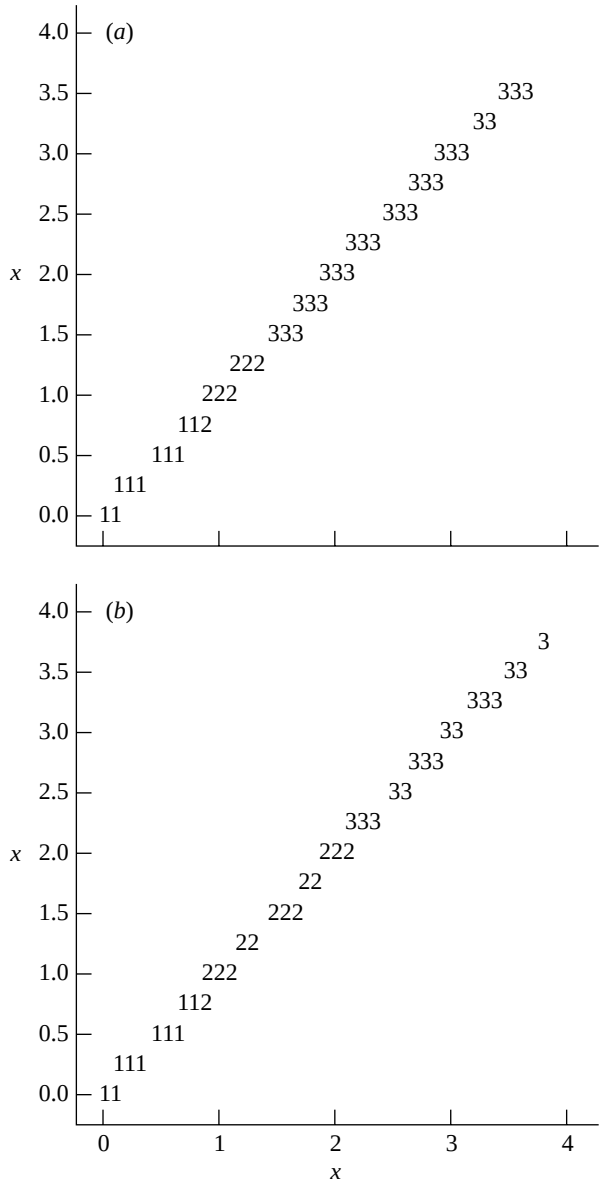

Figure 10. (*a*) Clusters suggested by the SAS MODECLUS procedure for the experimental data using a fixed kernel density estimation approach (extending kernel neighbourhood to two next-nearest neighbours) and a kernel radius $R = 0.4$. The three proposed clusters are delineated by numeric labels. Both axes of the diagram represent the same dimension, x, the one-dimensional distribution of the logarithmically transformed connection densities, as in figure 8; 133 of the data points are hidden in this representation. (*b*) Clusters suggested by the SAS MODECLUS procedure for the simulated data (random sample 7) using the same clustering approach and parameters as in (*a*). These data were randomly sampled from a continuous and monotonous distribution of theoretical values, yet produced results similar to the ones presented in part (*a*) of the diagram; 136 of the data points are hidden in this representation.

expected by sampling at random from a continuous monotonic distribution of connection densities.

Importantly, the absent connections were always in the same cluster as the weakest of the existing connections, for both the experimental and the simulated data. This means that no clear dividing line can be drawn between these two categories of connection densities on theoretical grounds.

We considered the possibility that the smooth distribution of densities may have arisen from the summation of several distinct distributions. A likely case in this event might have been that connections between identical area pairs in different animals formed characteristic individual distributions. We repeated the Monte Carlo simulations for the 32 connection means and medians derived from the grouped PMLS and PLLS cases. Medians were considered as an additional measure, because the detailed analyses by Scannell *et al*. (this issue) suggest a tendency of connection distributions to be non-normal and skewed. In a procedure analogous to the simulations described above, we fitted the histogram distribution of the experimental data (that is, the means or medians) with a smooth theoretical distribution (best fit was produced by a simple linear, monotonically decreasing function) from which we sampled randomly. The clusters detected in the experimental data were again similar to the groupings found in the simulated samples, and hence could be explained by the sampling process, rather than by a clustered distribution of connection densities. However, as the values for the means and medians were not very well defined by the small number of cases ($n_{\mathrm{PMLS}} = 5$, $n_{\mathrm{PLLS}} = 4$), the statistical results cannot be entirely conclusive, and further data will have to be analysed to confirm or reject these preliminary findings.

(d) *Relationships between areas size and connection density*

The preceding analyses demonstrated that there is a considerable range of connection densities in the cat's visual cortical network, as well as great variability in particular linkages across individual animals. Which factors influence connection density and variability? As figure 3 shows, there is also a considerable range of different area sizes, and a simple hypothesis would be that the strength of a connection is proportional to the size of the area from which it originates. The following analyses demonstrate that size does indeed matter.

Figure 11*a* shows the relationship between all relative areas sizes and the relative densities of connections originating from these areas (both for individual and averaged values). The averaged data (filled symbols) clearly show the influence of the area sizes on connection densities $R^2 = 0.54$; that is, the variability of the area sizes explains 54% of the variability of the relative connection densities. A similarly strong correlation ($R^2 = 0.67$) holds for the medians of the density data (not shown). We were concerned that the correlation might be unduly influenced by the two largest areas (areas 17 and 18) and their connections. Figure 11*b*, however, demonstrates that the correlations still held even when these areas were excluded.

The relative size of an area, therefore, is an important factor in determining the strength of connections it sends to other cortical regions, its variation accounting for more than 50% of the averaged densities' variation. Why should this be so? Neither relative nor absolute connection densities are strictly limited by the size of the originating area. Even relatively small areas are capable of sending dense connections (see figure 11). The answer may be related to the fact that cortical areas make a large number of connections with other areas in the network,

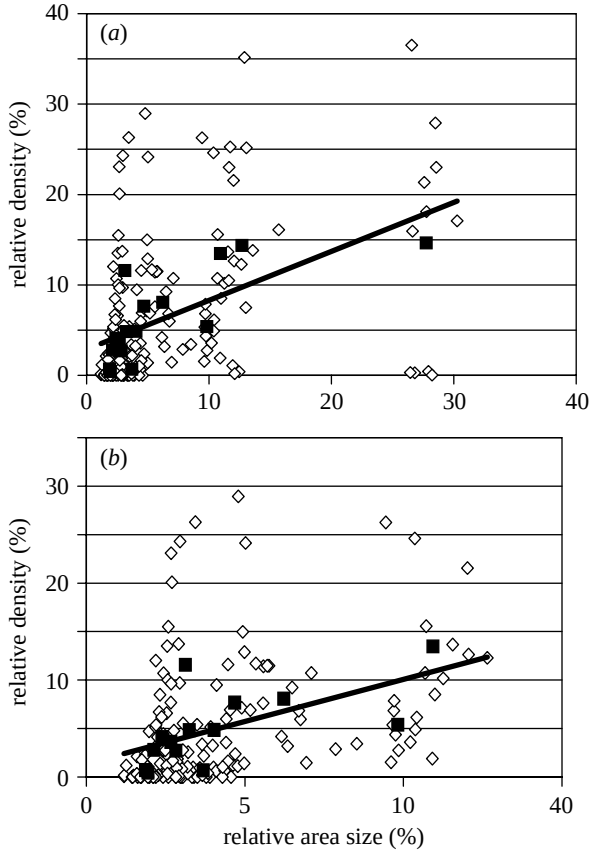

Figure 11. Relationship between relative area size and relative connection density for (*a*) all available data pairs and (*b*) all data except the pairs for primary cat cortical areas 17 and 18. Open symbols denote individual data points and black squares indicate averaged values. The equations and R^2-values for the linear line fit for the averaged data are (*a*) $y = 0.5398x + 2.876$, $R^2 = 0.5414$, (*b*) $y = 0.884x + 1.3101$, $R^2 = 0.4092$. The correlation for the medians of the densities, with the data for areas 17 and 18 excluded, was $R^2 = 0.44$.

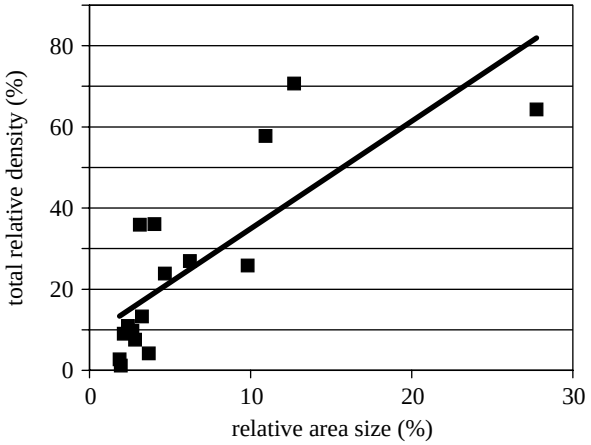

Figure 12. Relationship between relative area size and relative connection density of the sum of connections originating from an area. The densities were summed over all connections leading to areas 21a, AMLS, PMLS and PLLS (using the averaged values for the latter two cases). Superimposed is a linear regression curve with parameters $y = 2.6489x + 8.4443$, $R^2 = 0.616$.

and constraints might exist for the complete set of connections, rather than for any particular individual one. To explore this possibility, we calculated not the average, but the sum of densities for all connections that an area sends to other cortical regions. For example, in the case of area 17, we summed its average connection density to the four PLLS and five PMLS cases together with its relative densities to the individual 21a and AMLS cases. We also performed this process for the other 15 areas. Figure 12 shows the relationship between the relative area size and the relative summed connection density for all 16 areas. The diagram shows that the relative size of an area accounts for almost 62% of the variability in the total density of connections originating from it. An analogous calculation using median rather than mean values (not shown) confirms this picture, yielding a respective $R^2 = 0.61$. It has to be kept in mind, however, that we were only able to assess the outputs to four different cortical areas, rather than to all 16 areas in the networks. This raises the possibility that the correlation may have shown a different trend for a larger sample of targets (see § 4).

Despite the elements of uniform cortical organization revealed in the preceding results, figure 13 demonstrates that the connection patterns targeting individual areas can, nevertheless, be specific. This figure displays the correlation between relative area sizes and connection densities separated according to each of the four areas that were injected. While the densities of connections terminating in areas AMLS (figure 13*a*), 21a (figure 13*b*) and PMLS (figure 13*c*) follow the general correlation between area size and relative connection density (figure 11), those terminating in area PLLS (figure 13*d*) clearly do not. For area PLLS, it is predominantly the smaller areas that provide the strongest input, and any correlation between area size and connection density breaks down almost completely.

4. DISCUSSION

Counts of retrogradely labelled cortical neurons can provide a sound basis for quantifying several aspects of cortical systems connectivity. One important aspect relates to the subdivision of cortical regions (Van Essen 1985). Indeed, the initial motivation for undertaking this study was to evaluate the validity of various parcellation schemes for the MSS–LS cortex. There is little doubt that this region contains distinct medial and lateral bank territories, as they can be distinguished on the grounds of differences in their visuotopic organization (Palmer *et al.* 1978; Zumbroich *et al.* 1986; Grant & Shipp 1991), receptive field sizes and response properties (Von Grunau *et al.* 1987; Toyama *et al.* 1990), connectivity patterns (Symonds & Rosenquist 1984*a*; Sherk 1986) and perhaps even in their cytomyeloarchitecture (Sanides & Hoffmann 1969). In particular, in a previous neuroanatomical study involving counts of retrogradely labelled cells, Sherk (1986) was able to partition medial and lateral bank MSS areas based on a cluster analysis of their quantitatively distinctive thalamic and cortical inputs. The present study confirms and extends this finding by conclusively demonstrating, via independent statistical analyses (see table 1 and figure 13), that the two major subdivisions can be distinguished by their corticocortical connections alone.

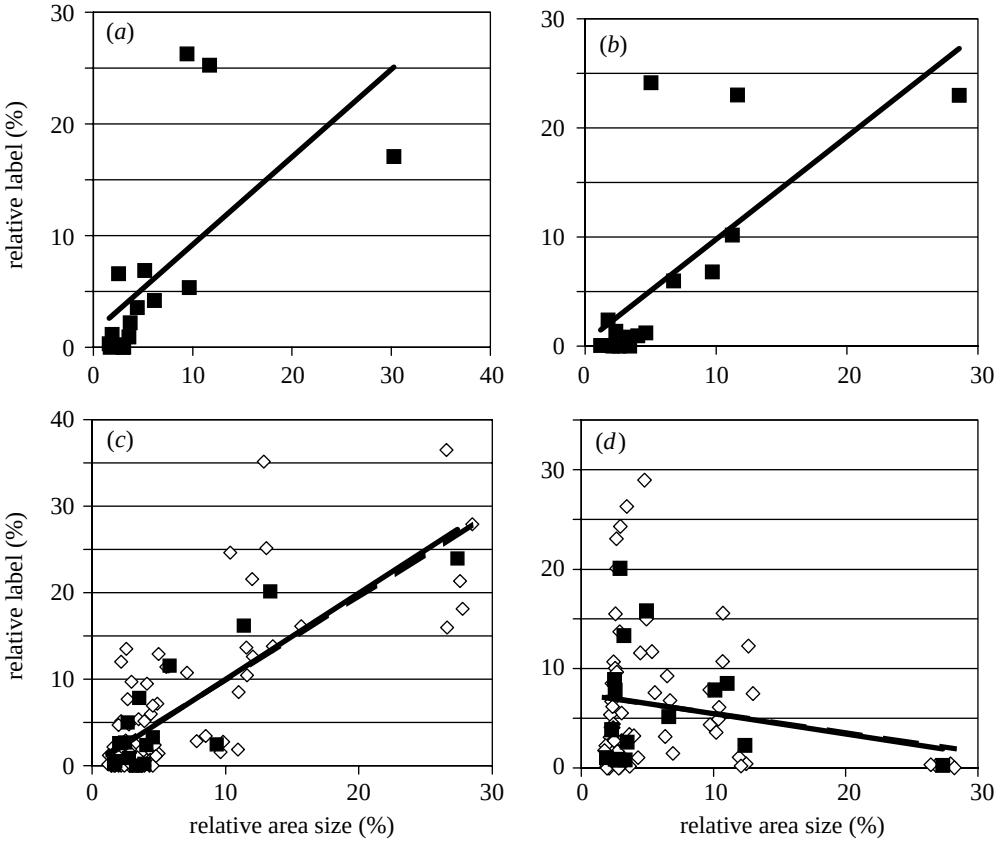

Figure 13. Correlation between relative area size and relative density of connections projecting to (*a*) AMLS, (*b*) 21a, (*c*) PMLS, (*d*) PLLS. Superimposed on the plots are regression curves that represent a linear fit of the data: (*a*) $y = 0.7844x + 1.3474$, $R^2 = 0.4061$, and (*b*) $y = 0.9431x + 0.3559$, $R^2 = 0.5141$. In the plots for the pooled cases PMLS (*c*) and PLLS (*d*), open symbols represent the individual and filled squares the averaged data. In these plots, the following equations represent the fit for the individual data: (*c*) $y = 0.978x + 0.1375$, $R^2 = 0.5781$, (*d*) $y = -0.196x + 7.4748$, $R^2 = 0.0328$. The averaged data are fitted linearly with the curves: (*c*) $y = 0.9943x + 0.0355$, $R^2 = 0.7472$, (*d*) $y = -0.2048x + 7.5301$, $R^2 = 0.0506$. If medians are used instead of means (not shown), almost identical R^2-values obtain $R^2 = 0.76$, for (*c*), and $R^2 = 0.05$, for (*d*).

There are, however, persistent disputes over the boundaries and the number of medial and lateral MSS areas. Palmer *et al.* (1978) and Symonds & Rosenquist (1984*a*) originally proposed that each bank contains a pair of separate areas, all confined within the MSS, and with the sulcul fundus demarcating the major boundary between them. There is now a broad consensus that Palmer *et al.*'s 'area PMLS' actually extends to the caudal pole of the lateral bank (see figure 1), where its main area centralis representation is located (Montero 1981; Sherk 1986; Updyke 1986; Grant & Shipp 1991). Some authors have also suggested that this area cuts across other boundaries proposed originally, including rostrally into area AMLS and caudally beyond the MSS to encompass all or part of area 21a on the adjoining posterior suprasylvian gyrus (Sherk 1986; Grant & Shipp 1991).

The results from the cluster analysis presented here have persuaded one of the authors (S.G.) to revise his opinion in respect to the possibility that area 21a is an integral part of PMLS. Despite their close proximity and their similar thalamic inputs (Grant & Shipp 1991), these areas can be clearly distinguished on the basis of their cortical inputs (table 1). The recent electrophysiological studies by Dreher *et al.* (1993, 1996) also presented compelling evidence that the two areas are functionally distinct.

The question of whether area PMLS also incorporates part of area AMLS remains open. Although two anterior medial bank injections (M01, M04) were adjoining and overlapping, their connectivity profiles were dissimilar to each other and to the profile of the PMLS (M03, M15, M17, M19) injections. This could lead to the conclusion that this region contains three distinct areas, a possibility entertained by Palmer *et al.* (1978). However, two confounding factors have to be considered. First, these anterior injections may have produced differential spread of tracer across their mutual boundaries and/or into neighbouring areas, so creating a mixed-area connectivity profile. Second, the more posterior of the two injections (M01) could have been placed mainly in PMLS, but in a part with a visuotopic organization that differed markedly from the region of the other PMLS injections. According to Grant & Shipp (1991) and Sherk & Mulligan (1993), this injection should encompass the lower visual periphery, whereas the other four injections were placed in the representation of more central vision. Support for this view comes from the observations that (i) the connection profile of injection M01 differed principally from the other four PMLS cases by the atypically dense input from area PS, which possesses only a lower field representation (Updyke 1986); and (ii) the case lacked input from areas 20a and 21a, which mainly

represent the upper visual and central field (Tusa & Palmer 1980).

These results reinforce the view that connectivity data have to be interpreted in conjunction with information about the visuotopic organization of the investigated cortical areas, especially of those with only partial visual field maps (Sherk 1986). A more detailed analysis of the structural organization of the LS region will be presented elsewhere. The following sections highlight general conclusions from the quantitative analysis of cortical systems connectivity.

(a) *Variability of anatomical connection strengths*

It is evident that the density of corticocortical connections can vary considerably across individual animals, even if the connections are between identical pairs of cortical areas. This great variability has been noted before by MacNeil *et al*. (1997), who also found that thalamocortical connections, by contrast, have very similar densities in different animals. The variability of corticocortical connection densities is intriguing, and potentially important both for the study of cortical organization and of cortical functions, since the latter are thought to be constrained by the anatomical strengths of connections.

We examined potential sources of this variability. By grouping together injections with similar connection profiles, we reduced the variance component that would have arisen simply from placing tracer in disparate and differentially connected cortical areas. Yet, much of the variability persisted. Since the injections in different animals did not cover exactly identical patches we can, however, not exclude the possibility that part of the remaining variability was still due to differential connectivity within the same cortical area; and Scannell *et al*. (this issue) present a more detailed discussion of this possibility. We also showed that the size of a cortical area contributes significantly to the average strength of connections originating from it. But as the relative and absolute sizes of areas were found to be largely invariant, this factor cannot be the main source of the connection strength variability. The variability we observed is unlikely due to be technical factors since MacNeil *et al*. (1997) have previously shown a similar order of variability in cats injected with different quantities of different neuroanatomical tracers and with a wide range of survival times. These authors have also presented cogent arguments that the striking differences in the variability of thalamocortical and corticocortical connections may be due to differences in the development of these two systems and the role of experience in shaping the final cortical connectivity patterns. A further detailed discussion of this topic is provided in the companion paper by Scannell *et al*. (this issue).

What are the practical consequences of the connectional variability? One obvious consequence is that conclusions derived from studies of connection densities in one or few animals should be treated with caution. Whereas thalamocortical connection densities, which show much less variation (MacNeil *et al*. 1997), may be adequately described by a singular value, corticocortical connection densities should be characterized as population values. The accuracy of such values can be roughly estimated by the following approach.

Consider the standard errors $s_{\bar{x}} = s/\sqrt{1}$ (where s is the standard deviation, n the number and $s_{\bar{x}}$ the standard error of the data) of the density data depicted in figures 5 and 6. Despite the relatively large variability of the single connections, expressed by the large standard deviations, the variability of the means for the densities, described by the standard errors, is less than $\pm 5\%$ of relative labelling. The means shown in these diagrams are calculated on the basis on $n_{\mathrm{PMLS}} = 5$ and $n_{\mathrm{PLLS}} = 4$ cases, respectively. This reiterates the point that the accuracy of the means, and their value as a defining measure for the density of a particular connection, increases with the number, n, of injection cases tested for the connection. What number of injections in different animals is required to define the density of a particular connection with sufficient accuracy? The above formula can be used for a first estimate of the number of cases required for the connections to PMLS and PLLS. As the standard error of the means only improves with the square root of the number of cases, very large numbers are required to achieve high accuracy. If one attempted to reduce the relative standard error (that is, $s_{\bar{x}}/\bar{x}$) to just 1% of the respective mean, not even 10 000 cases would be sufficient for some of the connections to PMLS or PLLS to achieve this goal. Numbers as high as these are, in any case, totally unfeasible for anatomical studies. On the other hand, if the goal was only to determine the density means with an accuracy of $\pm 5\%$ of the total cell labelling—an accuracy that is sufficient for the practical purpose of assigning densities to broad density categories—the number of cases considered here is already adequate. A practical estimate for the number of injection cases that are required and sufficient to study the density of corticocortical connections would, therefore, start at about five cases.

Our simple estimate is based on the assumption that the variation of densities around a mean can be approximated with a normal distribution. The study by Scannell *et al*. (this issue) demonstrates, on the basis of a larger number of pooled cases, that the variation is better described with an exponential distribution. This would make the mean even more difficult to predict from just a few cases. However, the authors also suggest that a broad classification of a particular corticocortical connection can be achieved by studying the connection in five to ten animals.

(b) *Classes of anatomical connection strengths*

Two important conclusions can be drawn from the Monte Carlo simulations presented in § 3(c). First, there is no inherent class structure in the distribution of connection densities and second, absent and very weak connections are inseparable. The latter conclusion makes immediate practical sense, as it is almost impossible to prove experimentally whether a connection appearing to be absent is in fact just very weak and so has avoided detection.

The first conclusion is significant for the description of cortical connectivity. If a categorization of connection densities is needed, it cannot be inferred from the structure of the data themselves, but rather has to be imposed on the observed densities. Instead of choosing such categories arbitrarily, however, we would suggest defining them relative to other features of cortical

organization. Because corticocortical connection strengths are strongly influenced by the size of the originating areas, descriptive categories of connection strengths might usefully incorporate these relationships and define connection strength relative to area size. A connection from a visual area could, for example, be defined as 'strong' if the relative proportion of retrogradely labelled cells in this area is equal to or exceeds the area's relative surface size, with respect to the remainder of the visual cortex. Naturally, the implementation of such an approach requires quantitative measures of connectivity and area dimensions.

Concepts for the evaluation of variable connection densities are also important for theoretical models of cortical function, which seek to relate the anatomical strength of different inputs to the functional influence that they may exert (e.g. Vanduffel *et al*. 1997). This is not to imply that any such anatomico-functional relationships are likely to be simple or direct ones, as the morphology and neurotransmitter contents of the cortical cells involved, their laminar origin and termination patterns, their synaptic distributions, their position within the local and global circuitry and so on may be of equal or greater functional consequence. Indeed, there are many precedents in this and other neural systems for believing that the numerical density of a particular connection (as defined in the present work) may be unrelated to its functional significance. Examples include the comparatively small impact of the strongest cortical inputs (from areas 17 and 18) on many of the response properties of area PMLS neurons (Spear & Baumann 1979; Guedes *et al*. 1983; Guido *et al*. 1990), and the singular, yet functionally powerful, climbing fibre input on to Purkinje cells of the cerebellar cortex (Ito 1984). Future studies will have to elucidate under which conditions the functional impact of a corticocortical connection is determined or restricted by its anatomical strength, and whether the variability of cortical connectivity in general has any significance for the functioning of the brain in individual animals. Again, however, progress in evaluating these questions will not be achieved until more quantitative data enter the analyses of cortical systems connectivity.

(c) *General constraints on projection densities*

We demonstrated that the size of a cortical area is strongly correlated with the average density of connections projecting from it, and even more strongly with the sum of all connections originating in the area. Since our data were founded on the distribution of retrogradely labelled cell bodies, the latter result can also be interpreted as a strong correlation between the size of an area and the total number of neurons within that area that make long-range projections to the rest of the cortex. Braitenberg & Schüz (1998) reviewed evidence from Bok (1959), Rockel *et al*. (1980) and Schüz & Palm (1989) indicating that the total number of neurons under one surface unit ($1\,mm^2$) of cortex is remarkably similar across different cortical areas in the same species. Beaulieu & Colonnier (1989) modified this hypothesis in that such constancy may only hold within particular cortical regions. They found that the number of neurons per $1\,mm^2$ column (NC) is smaller for cat motor areas than it is for visual areas. The binocular region of area 17 in turn has a higher NC than other visual cortical regions in the cat (Beaulieu & Colonnier 1985).

Our results suggest that a similar constancy may hold for the subgroup of neurons in an area that form long-range projections to other cortical regions. This would extend the notion put forward by Braitenberg & Schüz (1998) and other researchers that the mammalian neocortex possesses a structural uniformity, which varies only in respect to the quantity, and not the quality, of its features. For our data, this idea is exemplified by the contrast between the general constancy of long-range projection neurons per cortical surface unit and the highly specific PLLS projections, whose densities are unrelated to the dimensions of the originating areas. We therefore envision that cortical areas possess a relatively constant 'store' of projection neurons from which neurons can be allocated to particular connections according to the position and function of the areas in the cortical network. This view is encouraged by the finding of Beaulieu & Colonnier (1985) that the number of cells per cortical column in the supra- and infragranular layers (from which most long-range projections originate, including those to cat MSS cortex (Symonds & Rosenquist 1984*b*; Grant & Shipp 1991)) is more stable than in the granular layers, which may have an area-specific NC.

(d) *Limitations of the study*

Our approach attempted to improve the reliability of conclusions about cortical connectivity, compared to subjective, non-quantitative, evaluations of anatomical data. It was, however, also limited in a number of ways. We made great efforts to quantify the visual cortical connections projecting to the LS region, yet the data presented here were based on only a statistical sample ($<10\%$) of the total cell labelling present in all sections through the visual cortex in each cat. Moreover, the identified connections represented an incomplete, if large, set of all cortical connections of the LS region, as other inputs from limbic, cingulate, insular and frontal cortices were not included in the analyses. The MSS areas in turn constitute only one part of the considerably larger cortical network (Scannell *et al*. 1995). It must also be appreciated that cell counts alone can provide only a partial assessment of cortical connection densities, since wide variations in the size and morphology of cortical neurons (including their terminal arbors) may lead to differential labelling of their cell bodies, a difficulty further compounded by the general 'patchiness' of cortical systems connectivity. Additional information might have been gained by including anterograde data in our analyses, but objective quantification of terminal labelling densities in the cortex remain extremely problematic.

Our study had further, specific limitations. While the data provided a comprehensive sample of the visual cortical origins of MSS connectivity (from 16 different areas), only four substantially different MSS subdivisions were injected (table 2), two of which (areas 21a and AMLS) were represented only by individual cases. This particularly constrained the scope of our conclusions about the correlation between area size and cumulative densities of all originating connections and the suggested parcellation of anterior MSS cortex. Both issues clearly require further work.

Our observations regarding the constancy of area sizes were encouraging, given that there were some differences in the degree of shrinkage and in the precise section planes between individual brains. It is unfortunate, however, that, aside from the architectonically distinctive borders of areas 17 and 18, we can offer no independent verification of our methods for assigning most of the area boundaries. This is, of course, a recurring problem for all studies of cat extrastriate cortical areas, but we shall seek to verify the reliability of our parcellation elsewhere when we will consider the issue of visuotopic labelling patterns. With few exceptions (areas DLS/Peg, SVA and AEV), for example, there was clear evidence for correspondence between some area boundaries determined by gross anatomical landmarks and mirror-reversals in labelling progressions involving either the central-to-peripheral or upper-to-lower visual fields. Future approaches might also use the specific distribution of neurotransmitter and receptor systems (e.g. Gahr 1997; Geyer *et al*. 1997) to map out cortical areas; and the accuracy of two-dimensional representations of the folded cortical sheet might be improved with the help of computational optimization approaches (e.g. Drury *et al*. 1996).

Generally, to further evaluate aspects of the complex cortical connectivity revealed in this study, a wider-reaching computational approach to quantitative neuroanatomy will be required. Such an approach could combine traditional anatomical tracer experiments with the automated detection and quantification of labelled cells and terminals in sections, and the systematic compilation and databasing of the information, followed by statistical and computational analyses aimed at establishing global and specific features of cortical organization. Companion papers appearing in this issue (e.g. Hilgetag, Burns, O'Neill, Scannell & Young; Stephan *et al*.) hint at possible approaches for the various stages of such a project.

This study has been supported by a Wellcome Trust scholarship to C.-C.H. We thank Robert Taylor for his heroic contributions to the cell counts, Jack W. Scannell for brainstorming and clarifying discussions, and Malcolm P. Young, Bertram R. Payne, Gully A. P. C. Burns and Huw D. R. Golledge for helpful comments on the manuscript.

REFERENCES

Barone, P., Dehay, C., Berland, M., Bullier, J. & Kennedy, H. 1995 Developmental remodeling of primate visual cortical pathways. *Cerebr. Cortex* **5**, 22–38.

Beaulieu, C. & Colonnier, M. 1985 A comparison of the number of neurons in individual laminae of cortical areas 17, 18 and posteromedial suprasylvian (PMLS) area in the cat. *Brain Res.* **339**, 166–170.

Beaulieu, C. & Colonnier, M. 1989 Number of neurons in individual laminae of areas 3B, 4 gamma, and 6a alpha of the cat cerebral cortex: a comparison with major visual areas. *J. Comp. Neurol.* **279**, 228–234.

Bok, S. T. 1959 *Histonomy of the cerebral cortex*. Amsterdam: Elsevier.

Braitenberg, V. & Schüz, A. 1998 *Cortex: statistics and geometry of neuronal connectivity*. Berlin: Springer.

Coggeshall, R. E. & Lekan, H. A. 1996 Methods for determining numbers of cells and synapses: a case for more uniform standards of review. *J. Comp. Neurol.* **364**, 6–15.

Dreher, B., Michalski, A., Ho, R. H., Lee, C. W. & Burke, W. 1993 Processing of form and motion in area 21a of cat visual cortex. *Vis. Neurosci.* **10**, 93–115.

Dreher, B., Wang, C., Turlejski, K. J., Djavadian, R. L. & Burke, W. 1996 Areas PMLS and 21a of cat visual cortex: two functionally distinct areas. *Cerebr. Cortex* **6**, 585–599.

Drury, H. A., Van Essen, D. C., Anderson, C. H., Lee, C. W., Coogan, T. A. & Lewis, J. W. 1996 Computerized mappings of the cerebral cortex—a multiresolution flattening method and a surface based coordinate system. *J. Cogn. Neurosci.* **8**, 1–28.

Gahr, M. 1997 How should brain nuclei be delineated? Consequences for developmental mechanisms and for correlations of area size, neuron numbers and functions of brain nuclei. *Trends Neurosci.* **20**, 58–62.

Geyer, S., Schleicher, A. & Zilles, K. 1997 The somatosensory cortex of human: cytoarchitecture and regional distributions of receptor-binding sites. *NeuroImage* **6**, 27–45.

Grant, S. & Shipp, S. 1991 Visuotopic organization of the lateral suprasylvian area and of an adjacent area of the ectosylvian gyrus of cat cortex: a physiological and connectional study. *Vis. Neurosci.* **6**, 315–338.

Graybiel, A. M. & Berson, D. M. 1980 Histochemical identification and afferent connections of subdivisions in the lateralis posterior–pulvinar complex and related thalamic nuclei in the cat. *Neuroscience* **5**, 1175–1238.

Guedes, R., Watanabe, S. & Creutzfeldt, O. D. 1983 Functional role of association fibres for a visual association area: the posterior suprasylvian sulcus of the cat. *Exp. Brain Res.* **49**, 13–27.

Guido, W., Tong, L. & Spear, P. D. 1990 Afferent bases of spatial- and temporal-frequency processing by neurons in the cat's posteromedial lateral suprasylvian cortex: effects of removing areas 17, 18, and 19. *J. Neurophysiol.* **64**, 1636–1651.

Hilgetag, C.-C., Kötter, R. & Young, M. P. 1999 Interhemispheric competition of sub-cortical structures is a crucial mechanism in paradoxical lesion effects and spatial neglect. *Prog. Brain Res.* **121**, 125–146.

Ito, M. 1984 *Cerebellum and neural control*. New York: Raven.

Lennie, P. 1998 Single units and visual cortex organization. *Perception* **27**, 889–935.

Lomber, S. G., MacNeil, M. A. & Payne, B. R. 1995 Amplification of thalamic projections to middle suprasylvian cortex following ablation of immature primary visual cortex in the cat. *Cerebr. Cortex* **5**, 166–191.

MacNeil, M. A., Lomber, S. G. & Payne, B. R. 1997 Thalamic and cortical projections to middle suprasylvian cortex of cats: constancy and variation. *Exp. Brain Res.* **114**, 24–32.

Montero, V. M. 1981 Topography of the cortico-cortical connections from the striate cortex in the cat. *Brain Behav. Evol.* **18**, 194–218.

Musil, S. Y. & Olson, C. R. 1991 Cortical areas in the medial frontal lobe of the cat delineated by quantitative analysis of thalamic afferents. *J. Comp. Neurol.* **308**, 457–466.

Palmer, L. A., Rosenquist, A. C. & Tusa, R. J. 1978 The retinotopic organization of lateral suprasylvian visual areas in the cat. *J. Comp. Neurol.* **177**, 237–256.

Payne, B. R. 1993 Evidence for visual cortical area homologs in cat and macaque monkey. *Cerebr. Cortex* **3**, 1–25.

Rockel, A. J., Hiorns, R. W. & Powell, T. P. S. 1980 The basic uniformity in the structure of the neocortex. *Brain* **103**, 221–244.

Sanides, F. & Hoffmann, J. 1969 Cyto- and myelo-architecture of the visual cortex of the cat and of the surrounding integration cortices. *J. F. Hirnforsch.* **11**, 79–104.

Scannell, J. W., Blakemore, C. & Young, M. P. 1995 Analysis of connectivity in the cat cerebral cortex. *J. Neurosci.* **15**, 1463–1483.

Schüz, A. & Palm, G. 1989 Density of neurons and synapses in the cerebral cortex of the mouse. *J. Comp. Neurol.* **286**, 442–455.

Sherk, H. 1986 Coincidence of patchy inputs from the lateral geniculate complex and area 17 to the cat's Clare–Bishop area. *J. Comp. Neurol.* **253**, 105–120.

Sherk, H. & Mulligan, K. A. 1993 A reassessment of the lower visual field map in striate-recipient lateral suprasylvian cortex. *Vis. Neurosci.* **10**, 131–158.

Shipp, S. & Grant, S. 1991 Organization of reciprocal connections between area 17 and the lateral suprasylvian area of cat visual cortex. *Vis. Neurosci.* **6**, 339–355.

Spear, P. D. & Baumann, T. P. 1979 Effects of visual cortex removal on receptive-field properties of neurons in lateral suprasylvian visual areas of the cat. *J. Neurophysiol.* **42**, 31–56.

Symonds, L. L. & Rosenquist, A. C. 1984*a* Corticocortical connections among visual areas in the cat. *J. Comp. Neurol.* **229**, 1–38.

Symonds, L. L. & Rosenquist, A. C. 1984*b* Laminar origins of visual corticocortical connections in the cat. *J. Comp. Neurol.* **229**, 39–47.

Toyama, K., Fujii, K. & Umetani, K. 1990 Functional differentiation between the anterior and posterior Clare–Bishop cortex of the cat. *Exp. Brain Res.* **81**, 221–233.

Tusa, R. J. & Palmer, L. A. 1980 Retinotopic organization of areas 20 and 21 in the cat. *J. Comp. Neurol.* **193**, 147–164.

Tusa, R. J., Palmer, L. A. & Rosenquist, A. C. 1978 The retinotopic organization of area 17 (striate cortex) in the cat. *J. Comp. Neurol.* **177**, 213–235.

Updyke, B. V. 1986 Retinotopic organization within the cat's posterior suprasylvian sulcus and gyrus. *J. Comp. Neurol.* **246**, 265–280.

Vanduffel, W., Payne, B. R., Lomber, S. G. & Orban, G. A. 1997 Functional impact of cerebral connections. *Proc. Natl Acad. Sci. USA* **94**, 7617–7620.

Van Essen, D. C. 1985 *Functional organization of primate visual cortex*, vol. 3 (ed. A. Peters & K. Rockland), pp. 259–331. New York, London: Plenum Press.

Van Essen, D. C., Anderson, C. H. & Felleman, D. J. 1992 Information processing in the primate visual system—an integrated systems perspective. *Science* **255**, 419–423.

Von Grunau, M. W., Zumbroich, T. J. & Poulin, C. 1987 Visual receptive field properties in the posterior suprasylvian cortex of the cat: a comparison between the areas PMLS and PLLS. *Vis. Res.* **27**, 343–356.

Young, M. P. 1992 Objective analysis of the topological organization of the primate cortical visual system. *Nature* **358**, 152–155.

Zeki, S. & Shipp, S. 1988 The functional logic of cortical connections. *Nature* **335**, 311–317.

Zumbroich, T. J., Von Grunau, M., Poulin, C. & Blakemore, C. 1986 Differences of visual field representation in the medial and lateral banks of the suprasylvian cortex (PMLS/PLLS) of the cat. *Exp. Brain Res.* **64**, 77–93.